Journal of Materials Chemistry C

ROYAL SOCIETY OF CHEMISTRY

COMMUNICATION

View Article Online
View Journal | View Issue

Cite this: J. Mater. Chem. C, 2021, 9, 10226

Received 26th April 2021,
Accepted 28th July 2021

DOI: 10.1039/d1tc01928g

rsc.li/materials-c

Enhanced emission under proton stimuli based on a phenanthroimidazole derivative by switching the excited state type from the CT to the LE state†

Ying Zhang, *[a] Kai-Li Zhang,[a] Jun Liu,[a] Jun-Hao Wang, [b] Yao-Qin Feng,[a] Peng-Jun Deng,[a] Xinxin Tian, *[a] Gaoyi Han *[a] and Dan Li [c]

We report herein a vertical donor–acceptor-structured molecule based on a phenanthroimidazole derivative with rare enhanced emission under proton stimuli, which was caused by a change in the excited state type from the charge transfer state to the localized excited state. This provides a new strategy for developing off–on-type proton stimuli-responsive emitters requiring no stringent conditions for different states of being.

Stimuli-responsive luminescent materials dramatically change their emission color and/or intensity under external stimuli, and thus, there is a wide variety of potential applications for these materials as sensors for data memory and security.[1] There have been many reports describing advanced materials that respond to force,[2] light,[3] heat,[4] and vapor,[5] but not as much research has been conducted on proton-responsive materials. Many proton stimuli-responsive emitters exhibit a fluorescence redshift accompanied by a decrease in emission intensity. They are generally donor–acceptor (D–A) emitters containing moieties such as pyridine, pyrazine, and imidazole, which are easily bound to protons due to the presence of sp^2 hybrid nitrogen atoms with a strong alkaline property. This would reduce the electron density and support electron delocalization, leading to a redshift in absorption and fluorescence.

Non-irradiative decay methods utilizing a decreased energy gap result in proton-responsive emitters that exhibit notorious quenched emission with an on–off mode.[6] Thus, off–on mode proton-responsive emitters are rare, but appealing because they can provide a dual-mode switch with both color and intensity tuning and also will not emit false-positive signals upon quenching most interference after proton interaction.

Limited off–on types of proton-responsive emitters have been successfully obtained by strategies such as tuning the π–π interaction by configurational switching,[7] tuning of the S1–T1 intersystem crossing process (ISC) for strong phosphorescent emission,[8] blocking the photo-induced electron transfer (PET) process mode through pronounced stabilization of the localized frontier molecule orbits,[9] and enhancing two photon absorption (TPA) emission by tuning the intra-molecular charge/electron transfer process.[10] However, these were achieved using stringent conditions associated with inert atmospheres, specific stacked arrangements, and high intensity lasers. Thus, a new strategy is necessary to determine which materials could work under normal conditions.

In this work, (2*Z*,2′*Z*)-3,3′-(1,4-phenylene)bis(2-(4-(2-phenyl-1*H*-phenanthro[9,10-*d*]imidazol-1-yl)phenyl)acrylonitrile) (**M1**), which is an efficient off–on-type proton-responsive emitter, was synthesized through the Debus–Radziszewski reaction and Knoevenagel reaction.[2a] It was constructed with rigid phenanthroimidazole (PI) as a donor and orthogonally linked CNDSB as an acceptor at the N-1-imidazole position (Scheme 1 and Scheme S1, ESI†), which forms a perpendicular D–A conformation. **M1** exhibits dark emission in the original state, and off–on-responsive fluorescence with obvious blueshift emission

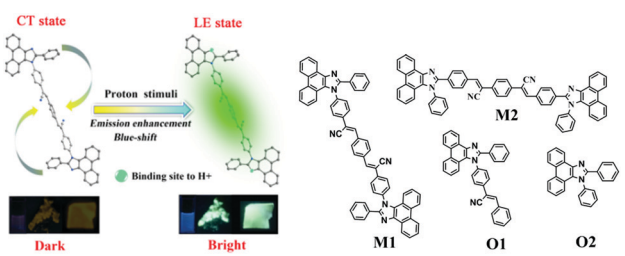

Scheme 1 A schematic diagram of the enhanced emission under proton stimuli of **M1** *via* tuning excited states upon the combination of protons and imidazole, and the molecular structures seen in this work.

[a] *Institute of Molecular Science, Innovation Center of Chemistry and Molecular Science, Shanxi University, Key Laboratory of Energy Conversation and Storage of Shanxi Province, Taiyuan 030006, P. R. China. E-mail: yzhang@sxu.edu.cn, han_gaoyis@sxu.edu.cn, tianxx@sxu.edu.cn*

[b] *Institute of Crystalline Materials, Shanxi University, Taiyuan 030006, P. R. China*

[c] *College of Chemistry and Materials Science, Jinan University, Guangzhou 510632, P. R. China*

† Electronic supplementary information (ESI) available. CCDC 1966223. For ESI and crystallographic data in CIF or other electronic format see DOI: 10.1039/d1tc01928g

under proton stimuli (Scheme 1). Additionally, **M1** exhibits a fast response and can function under varied conditions such as in solvent, in a nano-aggregation state, as a powder, and in a film state.

This has aroused our interest, and our careful investigation indicates that the proton-response mechanism varied from the charge transfer (CT) state to the localized excited (LE) state by the tuning of the electron density on the PI skeleton. This is different from the strategy of tuning *f* by changing the conformation, and provides a new strategy for off–on-type stimuli-responsive materials.

Acid vapor is harmful for human health and the environment, and thus, there is a need for acid-sensitive probes for the detection of volatile acids, such as trifluoroacetic acid (TFA). Note that this is different from pH-responsive materials responding to pH change, which can be realized by tuning the concentration of an acid solution, and with luminescent variation by protonation/deprotonation at the basic, acidic, or hydrogen-bonding sites on the molecules. We mainly investigated the emission response towards TFA vapor.

The as-synthesized solid **M1** powder was yellow in color, with an emission peak at 583 nm and a low quantum yield of 2.05%. After being fumed with TFA vapor, obvious emission transformation was observed, with a large blueshift of approximately 80 nm and a bluish-green emission peaking at 503 nm (Fig. 1a and Fig. S1, ESI†). The quantum yield increased to 7.53% with abnormal enhanced emission under proton stimuli, which is different from most reported redshifted compounds with quenched emission (Table S1, ESI†).[6] The emission can be recovered by NH_3 vapor fuming, and this process is reversible for at least 20 cycles (Fig. 1a and Fig. S2, ESI†). A response of blueshifted luminescence towards other acids also occurs in the solid state of **M1**, indicating its availability (Fig. S3, ESI†).

To explore the reason for the abnormal blueshift and enhanced emission under proton stimuli, first, we supposed that the stacking mode variation caused by proton stimuli leads to enhanced luminescence, as described in our previous report on a PI–CNS derivative.[2a] When the solid state of **M1** was fumed with TFA vapor over increasing time, powder X-ray diffraction (PXRD) patterns gradually changed from a satisfactory crystalline state into an amorphous state (Fig. S4a, ESI†), and the emission spectra blueshifted slowly from 583 nm to 503 nm (Fig. S5, ESI†). However, we cannot simply attribute the emission response to the variation in stacking and packing. Note that the amorphous state will form when the sample is exposed to TFA fuming or vigorous grinding (Fig. S4b, ESI†), but with different fluorescent behavior. For example, blueshift and enhancement of emission was observed after TFA fuming (Fig. S6a, ESI†) of either the original sample or the ground sample, while only a small redshift of the emission spectra was observed after strongly grinding the original sample or fuming it with TFA (Fig. S6b, ESI†). These results indicate that the packing mode does not have a critical effect on the fluorescence.

The above experimental results indicate that it should be the inherent electronic characteristics of this molecule and not the packing mode that mainly accounts for the blueshift and enhanced emission after acid stimuli. As expected, proton-responsive behavior was observed in a dilute solution state, nano-aggregation state, and film state that was similar to that observed in the solid powder state (Fig. 1b and Fig. S7–S10, ESI†). The spin-coated film (Fig. 1b) exhibited a blueshift and enhanced emission with a sensitive detection limit of 359 ppb and short response time of 0.51 s (Fig. S8 and S9, ESI†).

Subsequently, we investigated the photo-physical properties of **M1** to verify the origin of emission for the as-synthesized sample:

(1) The UV-Vis absorption and emission spectra of **M1** in different polar solvents were characterized. Its absorption spectrum shows nearly the same profile, exhibiting mainly two bands at 361 nm and 384 nm (Fig. S11, ESI†). The emission spectrum varied in different solvents (Fig. S12, ESI†). ha example, blue emission centered at 439 nm was observed for the sample in dimethylformamide (DMF). However, in tetrahydrofuran (THF), two emission bands appeared, with a new band emerging at longer wavelengths, at approximately 612 nm. The short-wavelength emission was nearly the same in varied solvents, while the emission at longer wavelengths was sensitive with different polar solvents. Note that the blueshift of **M1** in more polar DMF towards THF might occur because the oscillator strength (*f*) of the twisted D–A structure is too low, with only LE emission observed, while in THF, dual emission of both LE and CT was observed (as shown in the density functional theory (DFT) calculation section).[11a]

(2) The weak blue emission of **M1** in DMF peaked at 439 nm (Φ_f = not observed), while a relatively strong emission with a large redshift peaked at 568 nm (Φ_f = 5.81%) in the aggregation state as the water content increased (Fig. S13, S14 and Table S2, ESI†).[11b] Thus, aggregation-induced emission (AIE) was exhibited, and aggregation is preferable for the emission emerging in longer wavelengths.

(3) We examined the fluorescent lifetime of **M1** under various states and conditions. In THF solution, the lifetime at the long wavelength of 612 nm (1.89 ns) was longer than that at the short wavelength of 427 nm (0.77 ns) (Fig. S15 and Table S4, ESI†). **M1** will assume a well-dispersed nano-aggregation state in H_2O with an average size of approximately 79 nm, which can be proved by the dynamic light scattering (DLS) measurement (Fig. S10c, ESI†). In the nano-aggregation state, the lifetime was

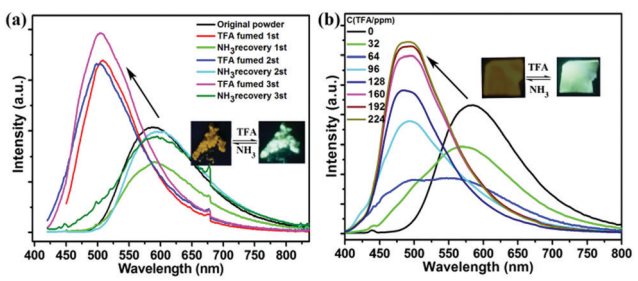

Fig. 1 Blueshift and enhanced emission after proton stimuli in the (a) powder state and (b) film state.

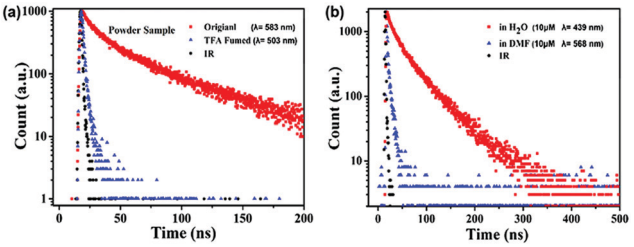

Fig. 2 Emission lifetime of **M1** (a) in a powder state before and after proton stimuli, and (b) at longer wavelengths in an aggregation state, and the short wavelength emission in DMF solvent.

measured as 42.96 ns at 568 nm, which is much longer than that measured for the blue emission in the dilute DMF solution (439 nm, 2.76 ns) (Fig. 2b and Table S3, ESI†). In the solid state, the fluorescent lifetime of the original 'dark' solid sample was measured to be 47.16 ns (at 583 nm), and it underwent a considerable decrease of 1.3 ns after protonation (at 503 nm) (Fig. 2a and Table S1, ESI†).

The sensitive emission towards different polar solvents as well as the long lifetime of longer wavelength emission in the solvent, aggregation, and solid powder state indicate that emission at longer wavelengths might originate from the CT state, although there was no CT absorption observed in the UV-Vis absorption spectrum, which was similarly observed in a previous work on a PI derivative (Table S1–S4, ESI†).[12] The disappearance of short wavelength emission and preferable long wavelength emission in the original solid powder and nano-aggregating sample in H_2O indicates that aggregation is beneficial for CT state generation for **M1**.

Acquiring an original 'dark' emitter is usually the first step in designing off–on-type stimuli-responsive luminescent materials. A dark emitter can be achieved through the mechanism of (i) strong π–π interaction with dense packing,[3,7] (ii) the ISC process,[2ab,8] (iii) the photo-induced electron transfer (PET) process of D–A molecules,[9,10] or (iv) charge transfer (CT) of the vertical D–A structure.[13,14] Of which, CT with a vertical D–A structure has not yet been reported for the designing of off–on-type proton-stimuli-response materials, although most proton-responsive emitters are D–A type molecules.[6]

Rationally, a vertical D–A molecule for 'dark' CT emission can be constructed based on PI derivatives due to their inherent characteristics: (i) the aromatic moiety at the N-1-imidazole position is always highly twisted towards the PI skeleton, as reported by us and other authors;[12,15] (ii) previous reports demonstrated that the excited state of a PI derivative can be changed from the LE state to a hybridized local and charge-transfer (HLCT) state with increased proportions of CT by attaching an electron-withdrawing moiety at the N-1-imidazole position of PI;[12] (iii) 1,4-bis(1-cyano-2-phenylethenyl)benzene (CNDSB) is considered to be a strong electron-withdrawing agent that contains an ethylene bond and cyano moiety, and connecting these at N-1-imidazole would probably construct a beneficial vertical D–A structure that can be used for the 'ultimate' CT state generation with 'dark' emission.

Furthermore, we measured the solid-state UV-Vis absorption spectra and electron spin resonance (ESR) spectra before and after TFA stimuli (Fig. S16, ESI†). A well-resolved profile of the UV-Vis spectra was obtained with absorption at 242 nm, 442 nm, and 471 nm for the original powder, while absorption at 442 nm and 471 nm disappeared for the TFA-fumed powder (Fig. S16a, ESI†). Additionally, as shown in Fig. S16b (ESI†), ESR was active for the original powder, indicating that the cation radical was generated for the D–A structure, and suggesting the existence of an intra-molecular charge-transfer process in the original powder.[13] The TFA-fumed powder was ESR silent, indicating the damage to the CT process after proton combination.

To prove that the 'dark' CT emission of **M1** indeed arose from the vertical D–A structure, reference compounds **O1**, **O2**, and **M2** were synthesized (Scheme 1 and Scheme S1, ESI†):

(1) **O1** was synthesized with a D–A structure similar to that of **M1**, and it also showed two emission bands mainly at 404 nm and 564 nm in THF solvent (Fig. S12c, ESI†), as well as an off–on proton stimuli-responsive luminescent property similar to that of **M1** (Fig. S1c, ESI†).

(2) After deleting the electron-acceptor part of CNDSB with a damaged D–A structure, the **O2** reference compound was obtained. As expected, longer wavelength emission was not observed at all. Only strong blue emission was observed that peaked at approximately 410 nm in various solvents and the solid state (Fig. S1d, S12d and Table S1, ESI†).

(3) **M2** was obtained by placing the electron-withdrawing part of CNDSB at the C-2-imidazole position, instead of on the N-1-imidazole position, as found in **M1**. As reported, it always exhibited a large conjugation structure with an aromatic moiety at the C-2-imidazole position of PI, which is not favorable for constructing a twisted vertical D–A structure.[15a] **M2** exhibits different fluorescent behavior from **M1** under TFA stimuli and is described as follows. (1) Although CNDSB is always considered as the AIE skeleton, connecting it at different positions on the PI derivative would result in emitters with much different emission efficiency. In contrast to 'dark' **M1** ($\Phi_f^{solution}$: not observed; Φ_f^{solid}:2.05%), **M2** shows strong emission in both solution (Φ_f = 10.51%) and the powder solid state (Φ_f = 12.13%). This result indicates that the 'dark' emission of **M1** cannot be simply attributed to the twisted structure of CNDSB. (2) **M2** shows a relatively small blueshift of 58 nm from 605 nm to 547 nm (80 nm for **M1** from 605 nm to 547 nm) (Fig. S1a and b, ESI†). Additionally, the solid state of **M2** shows a much shorter fluorescent lifetime of 4.93 ns at 605 nm compared with that of 47.16 ns at 583 nm for **M1**. These results indicate that the vertical conformation between D and A is very important for the fluorescent behavior of **M1**, and it can be obtained by attaching a strong acceptor at the N-1-imidazole position of the PI skeleton.

X-ray quality single crystals of **M1** have been obtained by diffusing methanol into the THF solution, which shows yellow colour emission and crystallized in the monoclinic *P*21/*c* group with a rod-like shape. As illustrated in Fig. S17a (ESI†), CNDSB shows small twisted angles of 12° between –CN against the benzene ring on N-1 imidazole, and 8° between the central benzene ring and the double bond, indicating the large conjugation of CNDSB.[11b] Two PI conjugations were connected with the planar belt of CNDSB, adopting a large twisted angle of

78°, which proved that a vertical structure was formed between the PI donor and the CNDSB acceptor.

The crystal structure analysis (Fig. S17b and c, ESI†) indicates that the molecules are mainly connected by C–H–π interactions between PI and CNDSB (2.71 Å, 2.78 Å and 2.88 Å). Obviously, there exists no π–π interaction for adjacent PIs (with a large distance of 5.3 Å and 5.6 Å,) and there exists neither obvious π–π interaction (9.01 Å) nor C–H–N interaction (3.6 Å) between the two CNDSBs, which would be beneficial for the entry of protons and thus explains the rapid response. As is known, the strong intermolecular π–π interaction of emitters often causes a redshift and decreased emission in the solid state,[16] and thus, the non-existent π–π interaction in this work proved that the blueshift of emission cannot be simply attributed to the damage of strong intermolecular π–π interaction.

Thus, the vertical structure of **M1** not only provides for the possibility of constructing a perpendicular D–A structure, but it also plays an important role in rapid response due to its unique twisted structure for the loose packing of **M1**.

The N-1-imidazole position can be considered as a proton combination site after acid stimuli due to the presence of bare N on it. To investigate the effect of the proton combination on the electronic properties and the conformational structure of **M1**, we measured the ^{1}H NMR before and after the addition of TFA to the test sample of **M1** (Fig. 3). The obvious chemical shift of H on PI was observed moving towards the lower field (red star signal), while that on CNDSB showed an undiscoverable chemical shift (blue point signal) (Fig. 3).

This result indicates that the proton affects the PI skeleton with a reduced electron density, but it does not affect the CNDSB skeleton at all.[6a] Additionally, the unchanged ^{1}H NMR result for CNDSB indicates that there was no obvious change in the twisted molecular structure between donor and acceptor after proton stimuli. This is reasonable because the strong repulsion of H on the benzene ring of N-1-imidazole towards the neighboring aromatic rings on PI restrains the obvious rotation under external stimuli.[6d,14]

As is known, the forbidden symmetry caused by the large twisted rotation between the donor and acceptor of D–A molecules was mainly responsible for the original 'dark' CT emission.[14] Tian *et al.* reported that AD-TPE is an off–on type of mechanic stimuli-responsive material with a vertical D–A structure, in which the emission turned on under mechanic stimuli by increasing the oscillator strength (*f*) of the CT state, but molecular conformational change was required. As suggested by the ^{1}H NMR characterization, the enhanced emission of the CT emitter under proton stimuli in this work should not be simply attributed to the change in the rotation degree between donor and acceptor, as described in previously reported works.[6d,14]

Furthermore, DFT calculation was performed to investigate the excited states of the molecule before and after protonation. Because the proton-responsive luminescent behavior depends on the inherent electronic character of the molecule, for simplicity, we chose single molecules derived from a single crystal structure for theory calculation. For the neutral molecule (Fig. 4a), (1) in the S1 state, the HOMO was mainly localized on the PI skeleton, while the LUMO was localized on the CNDSB skeleton, with a large separation of HOMO and LUMO. The vertical D–A structure was caused by the highly twisted conformation between PI and CNDSB devoid of a donor and acceptor spatially superimposable upon one another. This led to a weak Franck–Condon-allowed transition with oscillator strength of f = 0.0058, (i) indicating weak charge transfer from PI to CNDSB, which mainly contributes to the 'dark' CT emission, (ii) and also explained the unusually long emissive lifetime (original state, 47.16 ns).[6a] (iii) The small f also explained the absence of long-wavelength CT absorption. (2) The excited state of S5 (Fig. S18, ESI†) is permitted with a large f (1.9898), whose UV-Vis absorption peak is 429 nm, with the corresponding emission maximum calculated to be 502 nm. It was also noted that the excited states of S5, 20, 25, and 49 are of similar energy, and thus, they can be considered as one excited state, and they show a larger f value than that of S1 (Fig. S18, ESI†). This is consistent with the dual emission in some solvents following the anti-Kasha rule (Fig. S12a, ESI†),[17] suggesting that there are mainly two emission excited states for CT and LE for **M1**.

After protonation: (1) A reduced electron density on the PI skeleton was observed, resulting in the HOMO location shifting from the PI skeleton to the CNDSB skeleton (Fig. 4b), the excited state type changing from the CT state to the LE transition state, and the HOMO/LUMO orbitals being both localized

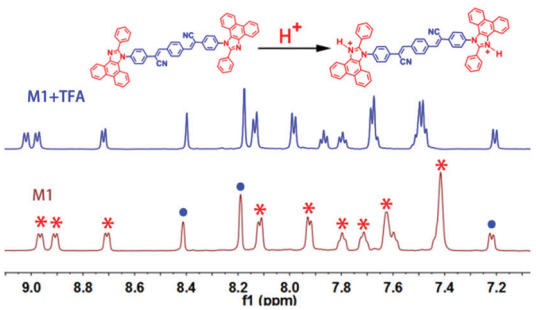

Fig. 3 The ^{1}H NMR spectra of **M1** in the original state and the protonation state (* denotes H on PI, and • denotes H on CNDSB).

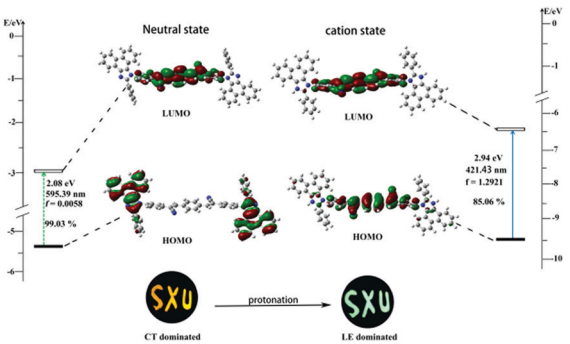

Fig. 4 The frontier orbital contributions of **M1** in a neutral state and protonation state estimated *via* the time-dependent DFT method (TD-DFT), and the corresponding proposed emission mechanism.

on the CNDSB skeleton. (2) The oscillator strength increased to $f = 1.291$, which was responsible for the enhanced emission. (3) The energy of the excited states of S1 (f = 1. 2921) and S3 (f = 0.8767) was very similar, and their absorption maximum was 421 and 414 nm, respectively, which can be considered as one excited state (Fig. S19, ESI†), with a corresponding emission at 493 and 480 nm, respectively. These DFT results as well as the increased energy gap verify the blueshift of the emission caused by protonation.

It should be noted that although it is common for protons to combine with an imidazole ring,[6a] such obvious difference in the excited state type after protonation is challenging. *E.g.*, the reference compounds of **M2** and **O2** cannot produce a turn-on luminescent response at all, indicating both the exquisite design of the vertical D–A structure and the sensitivity of the excited state caused by the inherent character of the PI derivative, which are vital for the abnormal enhanced emission under proton stimuli.

In summation, this work reports an elaborately designed 'off–on' type of proton-response luminescent material based on a PI derivative. Our approach is different from strategies described in previously reported works, where a simple tuning f of the CT state was performed *via* molecular conformation variation. Our method proved itself to be efficient for designing off–on-type stimuli-response materials *via* tuning the electron density on the donor part to change the excited state type of the vertical D–A structure, in which the vertical D–A structure with 'dark' CT emission and the sensitivity of the electron properties of the PI derivative are vital.

No special stacking modes are required, and this material can operate in an ambient environment under varied states, such as solution, nano-aggregation, film, and powder states, requiring no harsh conditions. This strategy will provide a new efficient method for developing off–on stimuli-responsive materials, in turn leading to the development of additional smart materials for applications in sensors, data memory, and security ink.

Conflicts of interest

There are no conflicts to declare.

Acknowledgements

This work was supported by the National Natural Science Foundation of China (No. 21602127, 22071138, 21701104 21731002, 21975104, 21903049) and the Fund for Shanxi ''1331 Project'' Key Innovative Research Team. The authors thank Prof. Jianbin Chao from the Scientific Instrument Center of Shanxi University for NMR measurement assistance.

Notes and references

1 (*a*) H. Sun, S. Liu, W. Lin, K. Y. Zhang, W. Lv, X. Huang, F. Huo, H. Yang, G. Jenkins, Q. Zhao and W. Huang, *Nat. Commun.*, 2014, **5**, 3601; (*b*) S. Yagai, S. Okamura, Y. Nakano, M. Yamauchi, K. Kishikawa, T. Karatsu, A. Kitamura, A. Ueno, D. Kuzuhara, H. Yamada, T. Seki and H. Ito, *Nat. Commun.*, 2014, **5**, 4013; (*c*) Z. Chi, X. Zhang, B. Xu, X. Zhou, C. Ma, Y. Zhang, S. Liu and J. Xu, *Chem. Soc. Rev.*, 2012, **41**, 3878; (*d*) R. Gao, X. Fang and D. Yan, *J. Mater. Chem. C*, 2019, **7**, 3399.

2 (*a*) Y. Zhang, Y. Q. Feng, X. Tian, J. H. Wang, H. Li, G. Han and D. Li, *Adv. Opt. Mater.*, 2018, **6**, 1800903; (*b*) W. Zhao, Z. He, Q. Peng, J. W. Y. Lam, H. Ma, Z. Qiu, Y. Chen, Z. Zhao, Z. Shuai, Y. Dong and B. Z. Tang, *Nat. Commun.*, 2018, **9**, 3044; (*c*) O. Sagara, S. Yamane, M. Mitani, C. Weder and T. Kato, *Adv. Mater.*, 2016, **28**, 1073; (*d*) K. Wang, Y. Xie, M. Liu, W. Tao, H. Zhang, M. Huang, J. You, Y. Liu, Y. Li, Z. Li and Y. Q. Dong, *Adv. Opt. Mater.*, 2020, **8**, 2000436; (*e*) Y. Yang, X. Fang, S. S. Zhao, F. Bai, Z. Zhao, K. Z. Wang and D. Yan, *Chem. Commun.*, 2020, **56**, 5267.

3 J. W. Chung, Y. You, H. S. Huh, B. K. An, S. J. Yoon, S. H. Kim, S. W. Lee and S. Y. Park, *J. Am. Chem. Soc.*, 2009, **131**, 8163.

4 A. Lavrenova, D. W. R. Balkenende, Y. Sagara, S. Schrettl, Y. C. Simon and C. Weder, *J. Am. Chem. Soc.*, 2017, **139**, 4302.

5 M. Zhang, G. Feng, Z. Song, Y. P. Zhou, H. Y. Chao, D. Yuan, T. T. Y. Tan, Z. Guo, Z. Hu, B. Z. Tang, B. Liu and D. Zhao, *J. Am. Chem. Soc.*, 2014, **136**(20), 7241.

6 (*a*) A. J. Zucchero, J. N. Wilson and U. H. F. Bunz, *J. Am. Chem. Soc.*, 2006, **128**, 11872; (*b*) Z. Yang, W. Qin, J. W. Y. Lam, S. Chen, H. H. Y. Sung, I. D. William and B. Z. Tang, *Chem. Sci.*, 2013, **4**, 3725; (*c*) P. Xue, P. Chen, J. Jia, Q. Xu, J. Sun, B. Yao, Z. Zhang and R. Lu, *Chem. Commun.*, 2014, **50**, 2569; (*d*) B. Shao, R. Jin, A. Li, Y. Liu, B. Li, S. Xu, W. Xu, B. Xu and W. Tian, *J. Mater. Chem. C*, 2019, **7**, 3263.

7 (*a*) Y. Ren, S. Xie, E. S. Grape, A. K. Inge and O. Ramström, *J. Am. Chem. Soc.*, 2018, **140**, 13640; (*b*) X. J. Zhou, C. Chen, C. X. Ren, J. K. Sun and J. Zhang, *J. Mater. Chem. C*, 2013, **1**, 744; (*c*) Y. Yang, X. Su, C. N. Carroll and I. Aprahamian, *Chem. Sci.*, 2012, **3**, 610.

8 W. Sun, Z. Wang, T. Wang, L. Yang, J. Jiang, X. Zhang, Y. Luo and G. Zhang, *J. Phys. Chem. A*, 2017, **121**, 4225.

9 M. S. Kwon, J. Gierschner, J. Seoa and S. Y. Park, *J. Mater. Chem. C*, 2014, **2**, 2552.

10 (*a*) H. J. Kim, C. H. Heo and H. M. Kim, *J. Am. Chem. Soc.*, 2013, **135**, 17969; (*b*) H. M. Kim, M. J. An, J. H. Hong, B. H. Jeong, O. Kwon, J. Hyon, S. C. Hong, K. J. Lee and B. R. Cho, *Angew. Chem., Int. Ed.*, 2008, **47**, 2231.

11 (*a*) Y. Tu, Y. Yu, D. Xiao, J. Liu, Z. Zhao, Z. Liu, J. W. Y. Lam and B. Z. Tang, *Adv. Sci.*, 2020, **7**, 2001845; (*b*) S. J. Yoon, J. W. Chung, J. Gierschner, K. S. Kim, M. G. Choi, D. Kim and S. Y. Park, *J. Am. Chem. Soc.*, 2010, **132**, 13675.

12 (*a*) S. Zhang, W. Li, L. Yao, Y. Pan, F. Shen, R. Xiao, B. Yang and Y. Ma, *Chem. Commun.*, 2013, **49**, 11302; (*b*) S. Zhang, Y. Dai, S. Luo, Y. Gao, N. Gao, K. Wang, B. Zou, B. Yang and Y. Ma, *Adv. Funct. Mater.*, 2017, **27**, 1602276.

13 Y. Hou, Y. Chen, Q. Liu, M. Liu, M. Yang, X. Wan, S. Yin and A. Yu, *Macromolecules*, 2008, **41**, 3114.

14 (*a*) Q. Qi, J. Qian, X. Tan, J. Zhang, L. Wang, B. Xu, B. Zou and W. Tian, *Adv. Funct. Mater.*, 2015, **25**, 4005; (*b*) I. Gómez, M. Reguero, M. B. Pasqua and M. A. Robb, *J. Am. Chem. Soc.*, 2005, **127**, 7119.

15 (*a*) Y. Zhang, S. L. Lai, Q. X. Tong, M. F. Lo, T. W. Ng, M. Y. Chan, Z. C. Wen, J. He, K. S. Jeff, X. L. Tang, W. M. Liu, C. C. Ko, P. F. Wang and C. S. Lee, *Chem. Mater.*, 2012, **24**, 61; (*b*) Y. Zhang, J. H. Wang, J. Zheng and D. Li, *Chem. Commun.*, 2015, **51**, 6350.

16 Y. Hong, J. W. Y. Lama and B. Z. Tang, *Chem. Commun.*, 2009, 4332.

17 H. Qian, M. E. Cousins, E. H. Horak, A. Wakefield, M. D. Liptak and I. Aprahamian, *Nat. Chem.*, 2016, **9**, 84.